CONF-900419--8

DE91 004458

DEVELOPMENT OF COATINGS WITH IMPROVED CORROSION RESISTANCE IN SULFUR-CONTAINING ENVIRONMENTS*

K. Natesan
Materials and Components Technology Division
Argonne National Laboratory
Argonne, IL 60439

and

R. N. Johnson
Westinghouse Hanford Company
Richland, WA 99352

DEC 0 4 1990

February 1990

The submitted manuscript has been authored by a contractor of the U. S. Government under contract No. W-31-109-ENG-38. Accordingly, the U. S. Government retains a nonexclusive, royalty-free license to publish or reproduce the published form of this contribution, or allow others to do so, for U. S. Government purposes.

DISCLAIMER

This report was prepared as an account of work sponsored by an agency of the United States Government. Neither the United States Government nor any agency thereof, nor any of their employees, makes any warranty, express or implied, or assumes any legal liability or responsibility for the accuracy, completeness, or usefulness of any information, apparatus, product, or process disclosed, or represents that its use would not infringe privately owned rights. Reference herein to any specific commercial product, process, or service by trade name, trademark, manufacturer, or otherwise does not necessarily constitute or imply its endorsement, recommendation, or favoring by the United States Government or any agency thereof. The views and opinions of authors expressed herein do not necessarily state or reflect those of the United States Government or any agency thereof.

Presented at the 17th International Conference on Metallurgical Coatings, San Diego, CA, April 2–6, 1990.

*Work supported by the U.S. Department of Energy, Advanced Research and Technology Development Fossil Energy Materials Program (WBS Elements ANL–3 and HEDL–2), under Contract W–31–109–Eng–38.

MASTER

DISTRIBUTION OF THIS DOCUMENT IS UNLIMITED

DEVELOPMENT OF COATINGS WITH IMPROVED CORROSION RESISTANCE IN SULFUR–CONTAINING ENVIRONMENTS*

K. NATESAN
Materials and Components Technology Division
Argonne National Laboratory, Argonne, IL 60439 (U.S.A.)

R. N. JOHNSON
Hanford Engineering Development Laboratory, Westinghouse Hanford Company, Richland, WA 99352 (U.S.A.)

Summary

Corrosion of metallic structural materials at elevated temperatures in complex multicomponent gas environments is a potential problem in many fossil energy systems, especially those using coal as a feedstock. The use of appropriate corrosion–resistant coatings on metallic components can minimize material degradation and extend component life. In the present study, the chemical compatibility of a number of coatings is examined by exposing them to simulated oxygen/sulfur mixed–gas environments at metal temperatures of 500 and 650°C. Coatings were developed via pack cementation and electrospark deposition techniques on T22 and T91 substrates. The oxidation/sulfidation test results for the coated specimens were compared with those for the uncoated alloys and for high–chromium structural alloys of interest in fossil energy applications.

1. Introduction

Earlier studies [1–3] of high–temperature corrosion of conventional engineering alloys and advanced nickel– and cobalt–base alloys showed significant sulfidation attack in environments with the low oxygen partial

---

* Work supported by the U. S. Department of Energy, Advanced Research and Technology Development Fossil Energy Materials Program (WBS Elements ANL–3 and HEDL–2) under Contract W–31–109–Eng–38.

pressures (pO_2) and moderate–to–high sulfur partial pressures (pS_2) that are typical of coal gasification and substoichiometric combustion systems. In these studies, extensive analyses were performed on the scales on several advanced alloys after exposure to simulated mixed–gas atmospheres; the reaction models were used to explain the behavior of these materials in the different regimes defined by the temperature and oxidant (O_2 and S_2) partial pressures. Process envelopes have been developed to depict the range of conditions under which different classes of materials exhibit acceptable corrosion performance. Improvements in corrosion resistance were also sought in a number of research programs to use the materials under lower pO_2 and higher pS_2 conditions and to prolong alloy performance before breakaway (accelerated) corrosion occurs.

The mechanism by which corrosion proceeds in a given alloy is strongly dependent on both alloy chemistry and oxygen/sulfur partial pressures in the exposure environment. Even if an alloy develops a protective oxide scale after short–term exposures to mixed–gas environments, the long–term behavior and thus the life expectancy of the alloy is strongly dependent on whether the alloy exhibits breakaway corrosion. Most of the alloys exhibit breakaway corrosion, especially in the oxygen/sulfur mixed–gas atmospheres typical of coal gasification and substoichiometric combustion processes. The exposure time at which breakaway corrosion occurs is dependent on temperature, gas chemistry, alloy composition, and scale microstructure [3,4].

Because the major objective in the development of corrosion– (sulfidation–) resistant alloys is formation of a slow–growing scale that is well bonded to the substrate alloy, research is underway to modify the surface regions of the alloy in order to enhance nucleation/growth of the oxide scale in the early stages of alloy exposure. The modifications produce both physical changes (e.g., grain size) and chemical changes (e.g., composition, grain boundary segregation, creation of metastable phases). One way to improve corrosion resistance of structural alloys is to apply a coating that is resistant to chemical and physical interactions with the hostile environment. In general, coating systems can be classified as either diffusion or overlay types: these are distinguished principally by the deposition method and the resultant coating/substrate bond structure. Among the numerous coating techniques, weld overlay, pack cementation, and electrospark deposition (ESD) processes have been examined for applications in heat recovery

units of coal conversion systems. In addition, plasma spray in either reduced pressure or vacuum and ESD techniques have been examined for improved erosion/corrosion resistance in gas turbine applications in combined–cycle plants.

In the present study, coatings developed via pack cementation and ESD were examined for their corrosion resistance in sulfur–containing atmospheres. In pack cementation, alloy samples are enclosed in a pack that consists of appropriate alloy powders, inert refractory powders, and a halide activator. The pack is heated to elevated temperature for a time sufficient to transport the desired coating elements from the pack to the alloy surface. Aluminizing, chromizing, and simultaneous chromizing and aluminizing coatings are prepared with this approach. The ESD process is a microwelding technique that uses short–duration, high–current electrical pulses to deposit an electrode material on a metallic substrate. A principal advantage of ESD is that the coatings are fused to a metal surface with a low heat input while the bulk substrate material remains at ambient temperature. This eliminates thermal distortions or changes in the metallurgical structure of the substrate. Because the coating is alloyed with the surface, i.e., metallurgically bonded, it is inherently more resistant to damage and spalling than the mechanically bonded coatings produced by most other low–heat–input processes (such as detonation–gun, plasma–spray and electrochemical plating). Fe–Cr–Mo coatings with and without bond coats, chromium carbide/Al coatings, and iron–aluminide coatings are prepared by ESD.

2. Experimental procedure

In the corrosion experiments described below, internally air–cooled ring specimens were used to simulate the heat exchanger tubes exposed in a coal–gasification type environment. A schematic diagram of the experimental setup is shown in Fig. 1. The experimental apparatus consists of a corrosion probe to which were attached ~16–mm–long ring specimens of different alloys with and without coatings. The probe was approximately 400 mm long and had a specially designed head that incorporated the coolant path and thermocouples. Temperature in the gas environment was measured by a Chromel/Alumel couple

inserted in the thermowell. Pt/Pt–Rh thermocouples were spot–welded onto the outer surfaces of ring specimens. At similar elevations on the corrosion probe, Chromel–Alumel couples were spot–welded on the inside surfaces of the specimens. In general, the metal temperature at the "fireside" was controlled to within 10 to 15°C of the desired value by adjusting the flow rate of the coolant. Flow rates of mixed gases such as $CO–CO_2–CH_4$ and $H_2–H_2S$ were adjusted through a gas flow system to achieve the desired oxygen and sulfur partial pressures in the reaction mixture. Two gas mixtures (identified as A and B) were selected for exposure of test specimens. Table 1 lists the room–temperature inlet compositions and the calculated compositions at several elevated temperatures. Also included in the table are the calculated oxygen and sulfur partial pressures at equilibrium in the exposure environment. The oxygen partial pressures established by test gas mixtures A and B were almost equal and corresponded to those in medium–Btu gasifiers, while the sulfur partial pressures of test gases A and B corresponded to ~4.4×10^{-8} and 1.0×10^{-6} atm, respectively, at a gas temperature of 871°C. Corrosion experiments were conducted at metal temperatures of 650 and 500°C, while the gas temperature was maintained at 871°C. Exposure time in different runs ranged from 500 to 2000 h.

In general, the test program was conducted with three objectives: (1) to evaluate the corrosion behavior of different coatings (applied on two different substrate alloys) in sulfur–containing environments, (2) to compare the performance of different coatings developed via pack cementation and EDS processes, and (3) to compare the corrosion rates for the coated alloys with those for uncoated structural alloys. Table 2 lists the alloys and coatings selected for the present study. Two different substrates, namely, T22 and T91 (with compositions of Fe–2 1/4Cr–1Mo and Fe–9Cr–1Mo) were used for the development of coatings. To assess the performance of coatings relative to the behavior of the high–chromium alloys, Alloy 800, 310 stainless steel, CR30A, and CR35A were also included. Upon completion of the exposures, cross sections of the ring specimens were examined with a scanning electron microscope (SEM) equipped with an energy–dispersive X–ray analyzer and an electron microprobe to identify morphological features and to establish the scale thickness and the depth of intergranular penetration of the substrate material.

3. Results and discussion

3.1. Base alloys

The tested metallic materials developed oxide or sulfide scales, depending on their chromium content, upon exposure to mixed-gas environments A and B at metal temperatures of 500 and 650°C. In general, an oxide mode of scaling (even though desirable) is rarely achieved in the low-pO2 and moderate-to-high-pS2 atmospheres at metal temperatures of interest in coal-gasification heat recovery systems. Even though development of fast-growing sulfide scales (especially in low–chromium ferritic steels) is the norm in these environments, the viability of an alloy for long-term service is dictated by the sulfidation rate; as a result, component temperatures must be kept low enough to maintain an acceptable scaling loss.

Figure 2 shows the corrosion scale morphologies and thicknesses observed on Fe-2 1/4Cr-1Mo and Fe-9Cr-1Mo ferritic steels and Type 310 austenitic stainless steel (SS) exposed at a metal temperature of 650°C to oxygen/sulfur mixed gas A for 500 h. The scales on the ferritic steels were predominantly Fe sulfide and (Fe,Cr) sulfide, while the Type 310 SS (typical of high-chromium alloys) developed thin oxide scales. The influence of gas chemistry variation (especially that of pS_2) was examined by exposing specimens to both gas mixtures. The results showed that the ferritic steels sulfidized in either of the gas mixtures and that sulfur partial pressure did not change the morphology of the corrosion-product layers. On the other hand, the high-chromium alloys exhibited a change in scaling morphology from oxide to sulfide, which eventually accelerated to catastrophic corrosion. Figure 3 shows the morphological features of Type 310 SS and Alloy 800 specimens after exposure to gas mixtures A and B. In gas mixture A, both alloys developed thin Cr oxide scales; Alloy 800 showed some intergranular penetration even after 500 h. In gas mixture B, Type 310 SS exhibited a thin oxide scale after 500-h of exposure; however, after 2000 h, the alloy developed a massive sulfide scale, thus indicating a tendency to undergo breakaway corrosion. Additional details on the corrosion behavior of different base alloys are published elsewhere [3,5].

Figure 4 shows corrosion loss for several base alloys at metal temperatures of 500 and 650°C after 2000 h of exposure to gas mixtures A and B. The results

show that the T22 alloy had corrosion losses of 2 and 3.3 mm/yr (based on linear kinetics) at 500°C in gas environments A and B, respectively; the corresponding metal losses at 650°C were 3.7 and >11.8 mm/yr in A and B, respectively. On the other hand, corrosion losses for high–chromium alloys ranged from 0.02 to 0.42 mm/yr (based on parabolic kinetics) over the temperature and gas chemistry conditions of the present tests. At 650°C, corrosion losses increased with the nickel content of the alloy, even though the higher–nickel alloys also contained higher levels of chromium.

3.2. Coatings on T22

A number of different coatings (see Table 2) were applied on T22 substrate alloy by both pack cementation and ESD. Of the nine coatings on T22 substrate, six were exposed for 2000 h to gas mixture B (with a higher sulfur partial pressure) at 500 and 650°C. Three of the coatings, (Fe_3Al with and without a bond coat, and an Al coating with Cr carbide bond coat) were exposed to the same environment for 500 h. Figures 5 and 6 show SEM photographs of corrosion scale morphologies observed on different coatings subsequent to exposure in gas mixture B at 500°C. The chromized, aluminized, and simultaneously chromized/aluminized coatings exhibit a substantial decrease in sulfidation attack and metal wastage via corrosion when compared with the uncoated T22 alloy. On the other hand, specimens with XF2020 coating (Fe–20Mo–20Cr–10Ni) with or without a refractory metal bond coat developed iron sulfide scales that were adherent to the substrate but almost as thick as in the uncoated T22 alloy. The Fe_3Al coating, with or without Nb-1Zr bond coat, exposed for 500 h to gas mixture B also exhibited iron sulfide scales of substantial thickness. A specimen with a chromized coating developed a thin Cr sulfide scale with a thickness that was only about 20% of that of the chromized layer. A specimen with an aluminized coating exhibited a thinner scale that contained Fe, Al, and S. The aluminized specimen with a bond coat of Cr carbide developed a somewhat thicker Fe sulfide scale, and Al in the coating had no effect on morphology or scale thickness. The aluminized coating applied via ESD was much thinner (~10 μm) than those applied with pack cementation (~200–400 μm). The simultaneously chromized/aluminized specimen developed a thin (Fe,Cr) sulfide scale, but the zone underneath the scale was enriched in Cr and Al and had virtually no Fe. This zone seems to act as a barrier to outward Fe transport, thereby minimizing sulfidation attack.

Figure 7 shows depth profiles of Fe, Cr, Al, Si, and S for chromized, aluminized, and ESD (with XF2020) T22 alloy specimens after exposure to gas mixture B for 2000 h at 500°C. The results show that the chromized and aluminized coatings resist sulfidation attack, while a coating of XF2020 has no resistance against sulfidation. The results also indicate that the presence of iron in the coating is conducive to sulfidation attack and formation of thick iron sulfide scales, especially in a substrate alloy that contains very little chromium, such as T22. Figure 8 compares the corrosion loss data obtained for T22 alloy in the uncoated condition with several different coatings after exposure to gas mixture B at 500 and 650°C. The data for the Fe_3Al- and Cr-carbide/Al coated specimens were obtained after 500 h of exposure, while those for the others were obtained after 2000 h of exposure. The results show substantial improvement for the pack cementation coatings and the ESD Cr carbide/Al coating in these reducing environments. A comparison of the corrosion loss data in Fig. 8 with those for the high–chromium base alloys in Fig. 4 indicates that the rates for pack cementation coatings on T22 are similar to or lower than those for the base alloys.

3.3. Coatings on T91

Three different coatings were applied to the T91 substrate by pack cementation and exposed for 500 h to oxygen/sulfur mixed-gas atmospheres at 500 and 650°C. Figures 9 and 10 are SEM photographs of T91 specimens exposed at 500 and 650°C, respectively, in the uncoated condition and with chromized, aluminized, and simultaneously chromized/aluminized coatings. The uncoated alloy developed a two–layer scale with a predominantly Fe sulfide outer layer and an (Fe,Cr) sulfide inner layer. On the other hand, the coated specimens exhibited much thinner corrosion product layers even though they contained Fe, S, and Cr and/or Al. Penetration of the alloy in the coated specimens was also small even when exposed at 650°C.

Figure 11 shows elemental depth profile analyses for the chromized, aluminized, and simultaneously chromized/aluminized coatings after 500 h of exposure to gas mixture B at 650°C. The results indicate that increased chromium and/or aluminum concentration is beneficial in resisting sulfidation attack, but that the integrity of the coating is strongly dictated by mechanical properties and by adhesion of the coating to the substrate rather than by chemical interactions with the exposure environment. Figure 12 shows scale thickness

and penetration data for the T91 alloy in uncoated condition and with different coatings after 500 h of exposure in gas mixture B at 650 and 500°C. For the uncoated alloy, corrosion losses (scale thickness plus penetration) at 500 and 650°C were ~100 and 600 μm, respectively, which translate to ~1.75 and 10.5 mm/yr, based on linear kinetics for the corrosion process. On the other hand, the chromized and chromized/aluminized coatings performed significantly better than the base alloy. Scale thicknesses were substantially lower (e.g., 40 μm, for a rate of 0.7 mm/yr at 650°C) at both exposure temperatures. The aluminized coating exhibited somewhat poorer performance in terms of void formation and cracking, which might have resulted during the fabrication of the coating rather than during exposure in the mixed–gas atmospheres.

4. Conclusions

Several coatings were developed via pack cementation and ESD coating techniques on two different low–chromium substrate materials (T22 and T91 alloys). The uncoated and coated specimens were exposed to oxygen/sulfur mixed–gas atmospheres at metal temperatures of 500 and 650°C for time periods of 500 and/or 2000 h. The results showed that uncoated alloys exhibited unacceptable corrosion rates via sulfidation at both temperatures after exposure to environments containing low oxygen and moderate–to–high sulfur partial pressures. On the other hand, pack cementation coatings exhibited substantial reductions in sulfidation rate under the same conditions. Some of the ESD coatings, such as Fe_3Al with or without bond coat and Cr carbide–aluminized coating, showed somewhat lower corrosion loss than the uncoated alloy. However, the coating thicknesses and compositions must be optimized to improve their sulfur resistance in mixed–gas atmospheres.

Acknowledgments

This work was supported by the U.S. Department of Energy, Advanced Research and Technology Development Fossil Energy Materials Program, Work Breakdown Structure ANL–3 and HEDL–2, under Contract W–31–109–Eng–38. D. L. Rink assisted with the corrosion test program conducted at Argonne National Laboratory.

References

1. K. Natesan, Corrosion and Mechanical Behavior of Materials for Coal Gasification Applications, Argonne National Laboratory Report ANL–80–5, May 1980.
2. T. C. Tiearney, Jr., and K. Natesan, Oxid. Met., 17 (1982) 1.
3. K. Natesan, Corrosion (Houston), 41 (1985) 646.
4. K. Natesan, in M. A. Dayananda, S. J. Rothman, and W. E. King (eds.), Symposium on Oxidation of Metals and Associated Mass Transport, TMS–AIME, 1987, p. 161.
5. K. Natesan, in W. T. Bakker, S. Dapkunas, and V. Hill (eds.), Proc. Conf. Materials for Coal Gasification, ASM International, 1987, p. 51.

Table 1. Gas compositions (in vol.%) and oxygen and sulfur partial pressures (in atm) used in test program

Gas Parameter	Gas Mixture A				Gas Mixture B			
	20°C	500°C	650°C	871°C	20°C	500°C	650°C	871°C
Composition								
CO	22.3	4.5	31.4	44.5	21.8	4.5	31.0	43.9
CO_2	44.7	50.7	31.6	20.3	43.7	49.2	30.7	19.7
CH_4	7.4	3.7	1.4	<0.1	7.3	3.8	1.4	<0.1
H_2	25.4	12.9	23.8	22.9	26.2	13.1	24.3	23.4
H_2O	–	28.0	11.7	12.1	–	28.2	11.7	12.2
H_2S	0.21	0.25	0.19	0.17	1.02	1.22	0.94	0.85
Partial Pressure (atm)								
p_{O_2}	–	9.5×10^{-28}	1.2×10^{-23}	3.9×10^{-18}	–	9.2×10^{-28}	1.2×10^{-23}	3.8×10^{-18}
p_{S_2}	–	3.3×10^{-11}	5.0×10^{-10}	4.4×10^{-8}	–	7.7×10^{-8}	1.0×10^{-6}	1.4×10^{-5}

Table 2. Details on alloy/coatings used in the present studies

Alloy/Coating	Composition	Coating Method
T22	Fe-2 1/4Cr-1Mo	-
T91	Fe-9Cr-1Mo	-
Alloy 800	Fe-32.5Ni-21Cr	-
310 SS	Fe-25Cr-20Ni	-
CR35A	45Ni–37Cr–Fe	-
CR30A	51Ni–31Cr–2Mo–Fe	-
T22/Fe_3Al	T22/Fe-15Al	ESD
T22/Nb-1Zr/Fe_3Al	T22/Nb-1Zr/Fe–15Al	ESD
T22/XF2020	T22/Fe-20Mo-20Cr-10Ni	ESD
T22/KBI10/XF2020	T22/Ta-10W/XF2020	ESD
T22/KBI41/XF2020	T22/Ta-37.5Nb-2.5W/XF2020	ESD
T22/C 815/Al	T22/Cr Carbide/Al	ESD
T22/Chromized	T22/Cr	Pack Cementation
T22/Aluminized	T22/Al	Pack Cementation
T22/Cr/Al	T22/Cr+Al	Pack Cementation
T91/Chromized	T91/Cr	Pack Cementation
T91/Aluminized	T91/Al	Pack Cementation
T91/Cr/Al	T91/Cr+Al	Pack Cementation

Figure Captions

Figure 1. Schematic of laboratory setup used for corrosion evaluation of coating materials.

Figure 2. Corrosion scale morphologies in several ferritic and austenitic Fe–base alloys at a metal temperature of 650°C after exposure to gas mixture A at 871°C.

Figure 3. Effect of gas chemistry and exposure time on corrosion morphologies of two austenitic alloys.

Figure 4. Corrosion loss in several base alloys after 2000–h exposure to gas mixtures A and B at metal temperatures of 500 and 650°C.

Figure 5. SEM micrographs of uncoated and coated T22 alloys after 2000–h exposure to gas mixture B.

Figure 6. SEM photograph of T22 alloy with three different ESD coatings after 500–h exposure to gas mixture B.

Figure 7. Elemental depth profiles for chromized (left), aluminized (middle), and XF2020-coated (right) T22 alloy after 2000–h exposure to gas mixture B at 500°C.

Figure 8. Corrosion loss data for T22 alloy in uncoated condition and with several coatings after 2000–h (unless marked otherwise) exposure to gas mixture B at 500 and 650°C.

Figure 9. SEM micrographs of uncoated and coated T91 alloys after 500–h exposure to gas mixture B at 500°C for 500 h.

Figure 10. SEM micrographs of uncoated and coated T91 alloys after 500–h exposure to gas mixture B at 650°C for 500 h.

Figure 11. Elemental depth profiles for chromized (left), aluminized (middle), and simultaneously chromized/aluminized (right) T91 alloy after 500–h exposure to gas mixture B at 650°C.

Figure 12. Corrosion loss data for T91 alloy in uncoated condition and with several coatings after 500 h of exposure to gas mixture B at 500 and 650°C.

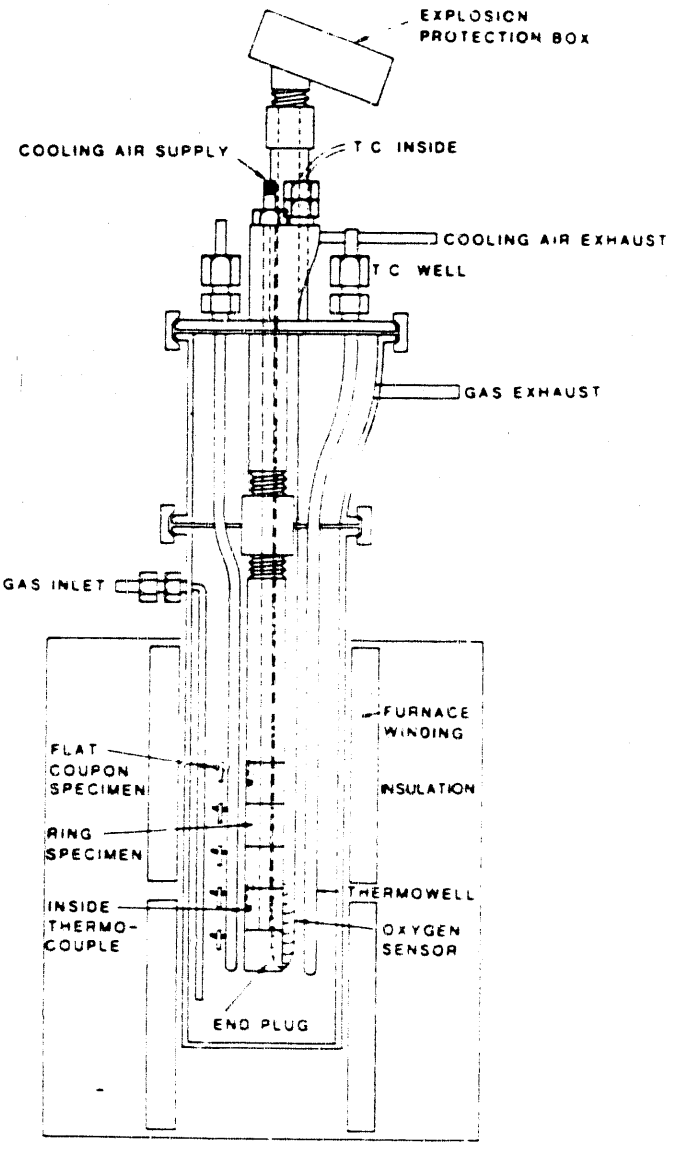

Figure 1. A schematic of the laboratory setup used for the corrosion evaluation of coating materials.

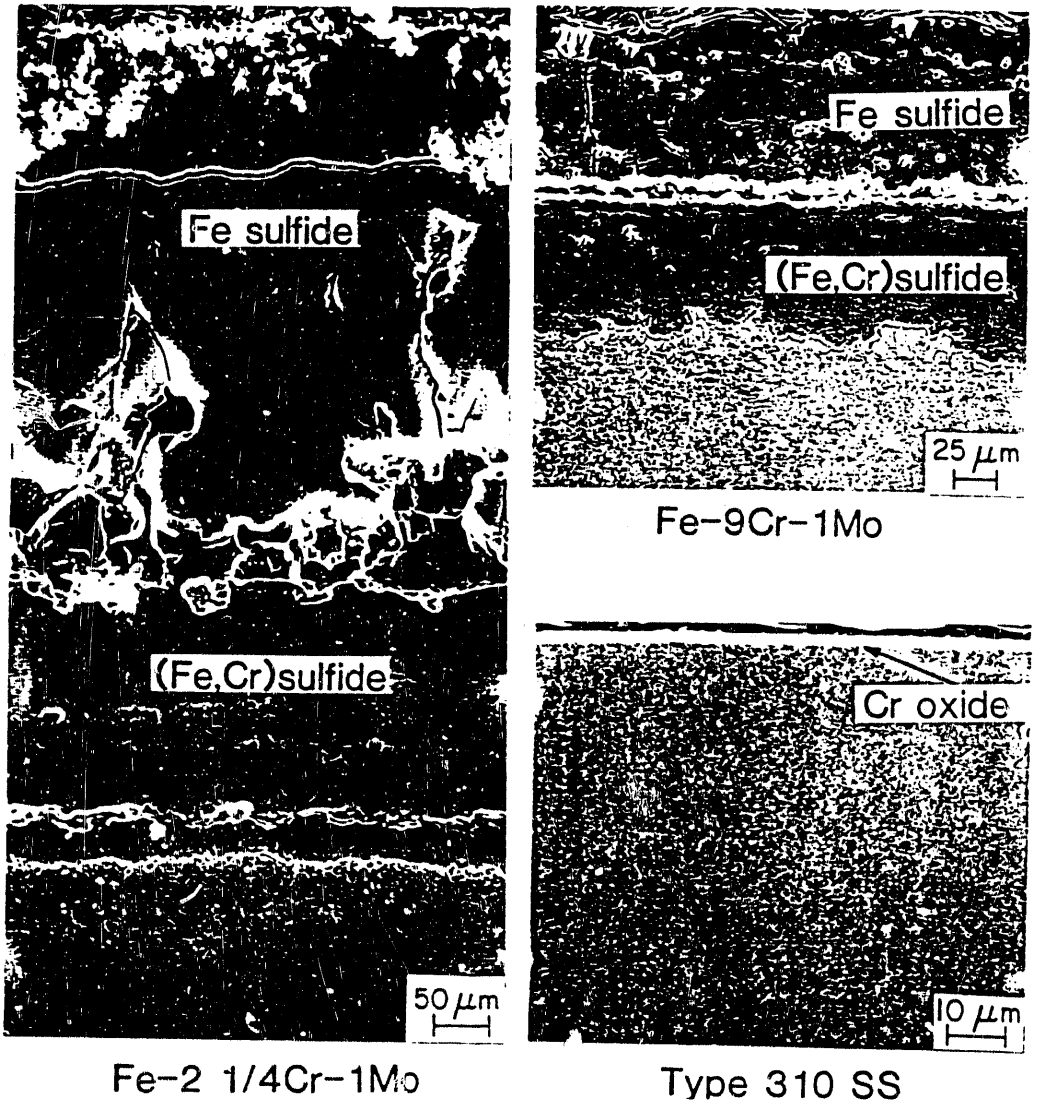

Figure 2. Corrosion scale morphologies in several ferritic and austenitic Fe-base alloys at a metal temperature of 650°C after exposure to gas mixture A at 871°C.

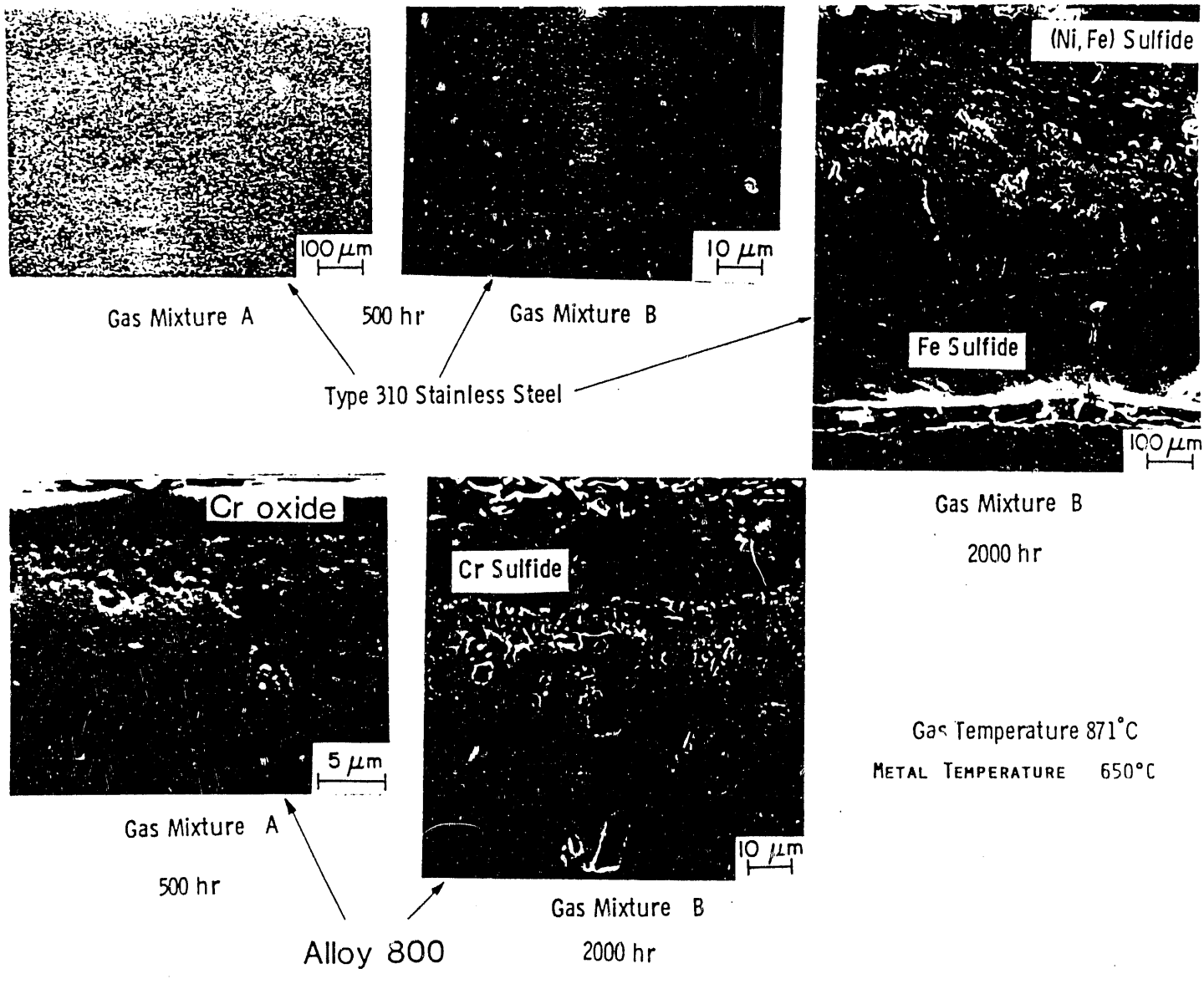

Figure 3. Effect of gas chemistry and exposure time on the corrosion morphologies of two austenitic alloys.

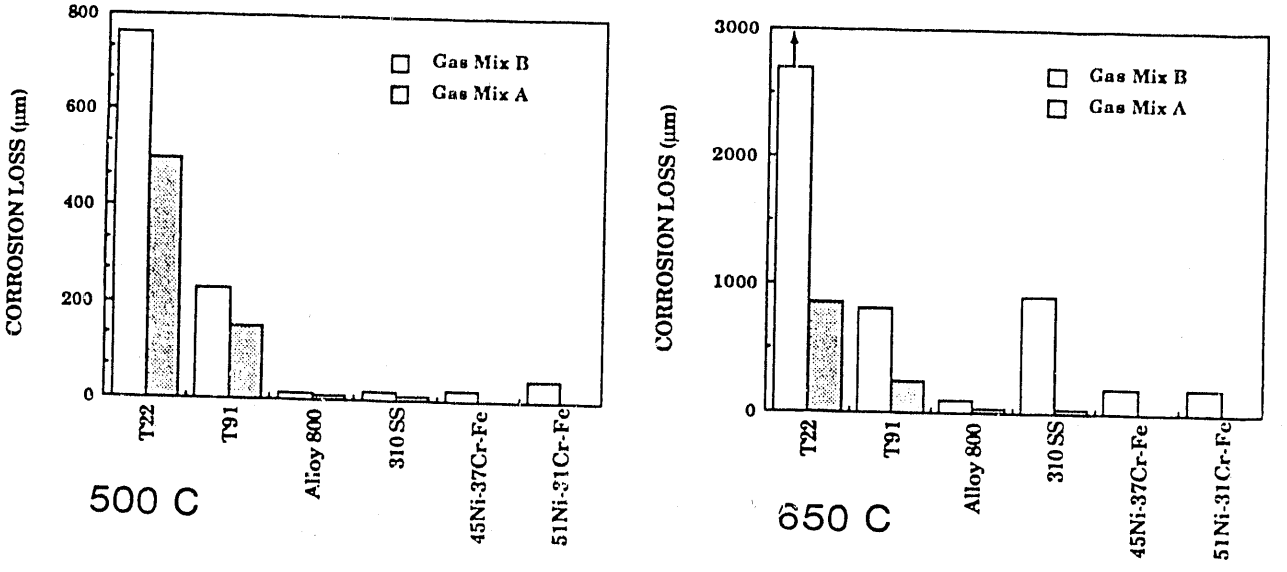

Figure 4. Corrosion loss data for several base alloys after 2000 h exposure to gas mixtures A and B at metal temperatures of 500 (left) and 650°C (right).

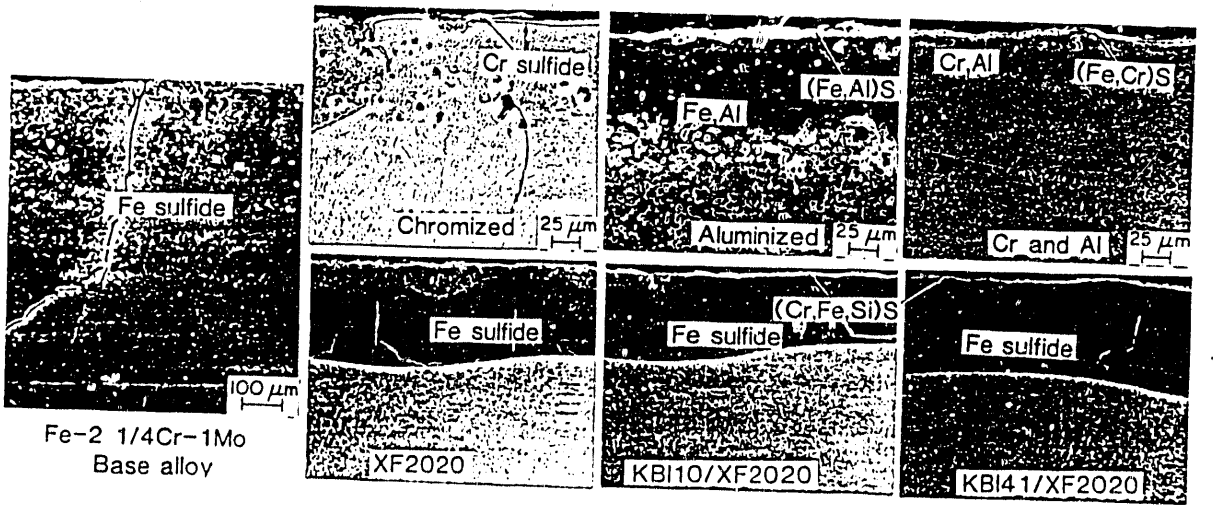

Figure 5. SEM micrographs of uncoated and coated T22 alloys after 2000 h exposure to gas mixture B.

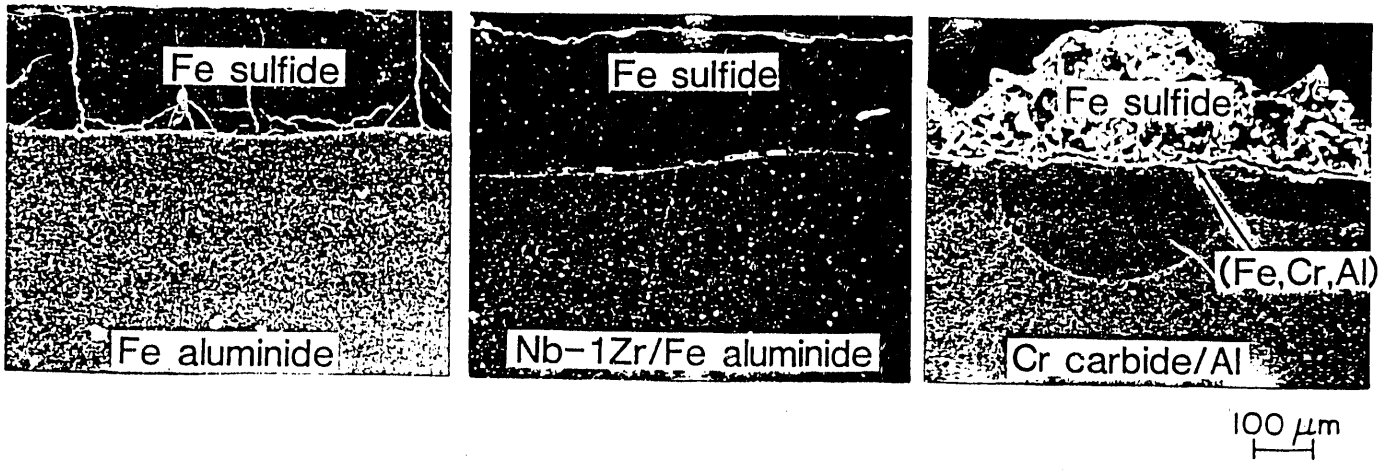

Figure 6. SEM photograph of T22 alloy with three different ESD coatings after 500 h exposure to gas mixture B.

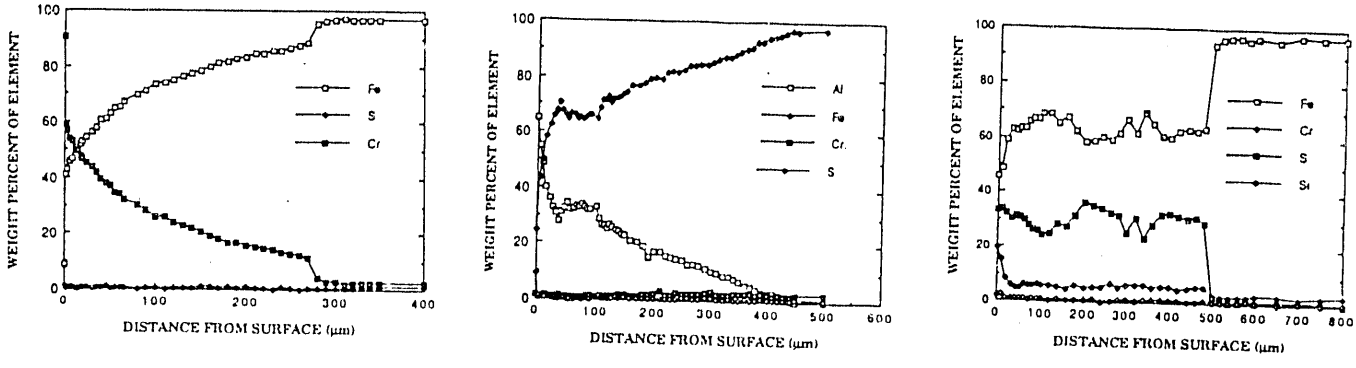

Figure 7. Elemental depth profiles for chromized (left), aluminized (middle), and XF2020-coated (right) T22 alloy after 2000 h exposure to gas mixture B at 500°C.

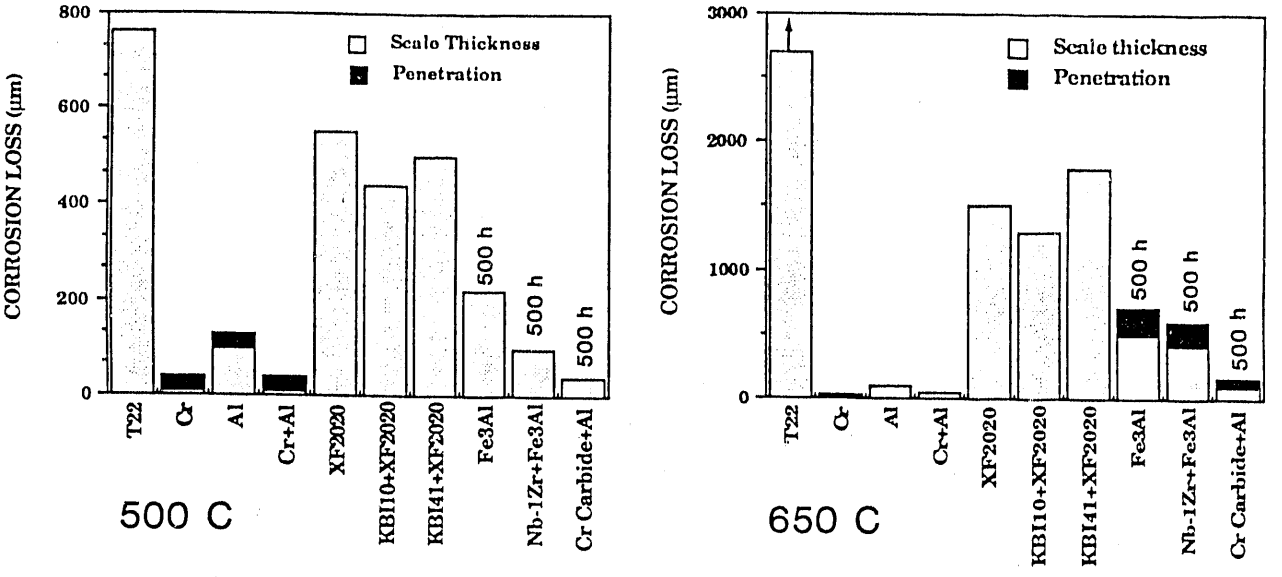

Figure 8. Corrosion loss data for T22 alloy in the uncoated condition and with several coatings after 2000 h (unless marked otherwise) exposure to gas mixture B at 500 and 650°C.

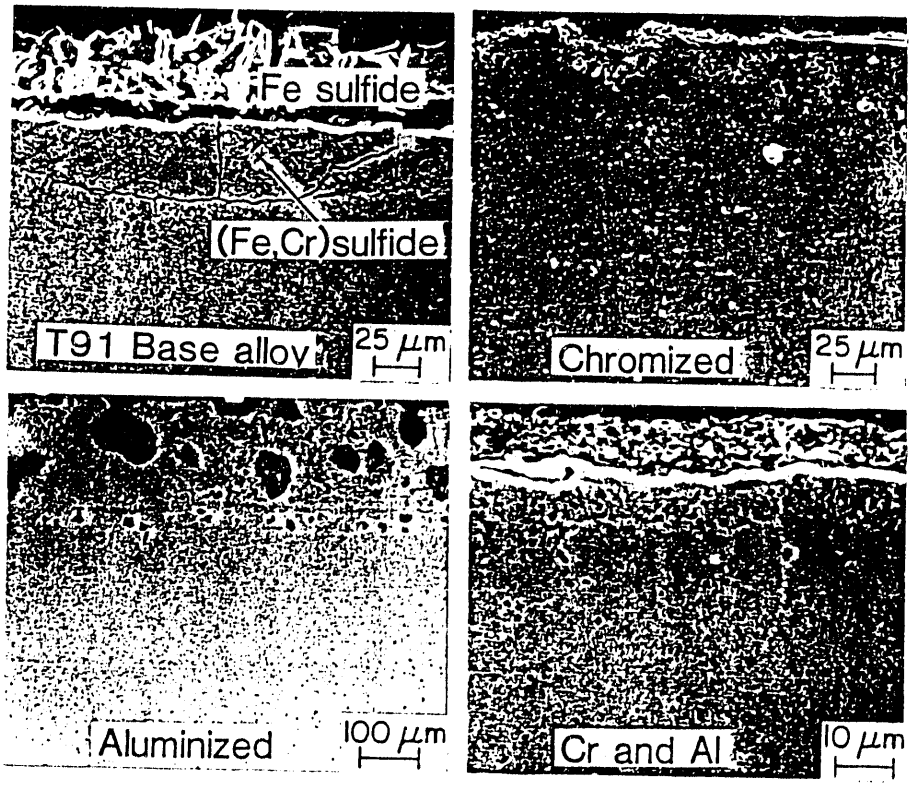

Figure 9. SEM micrographs of uncoated and coated T91 alloys after 500 h exposure to gas mixture B at 500°C for 500 h.

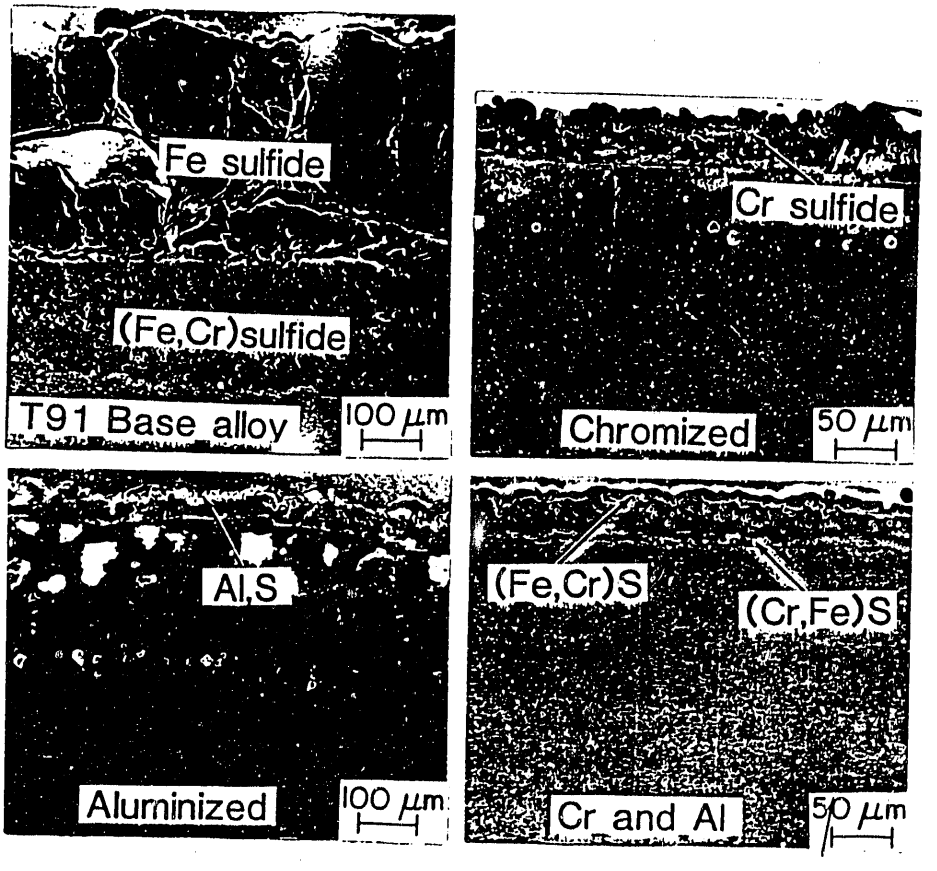

Figure 10. SEM micrographs of uncoated and coated T91 alloys after 500 h exposure to gas mixture B at 650°C for 500 h.

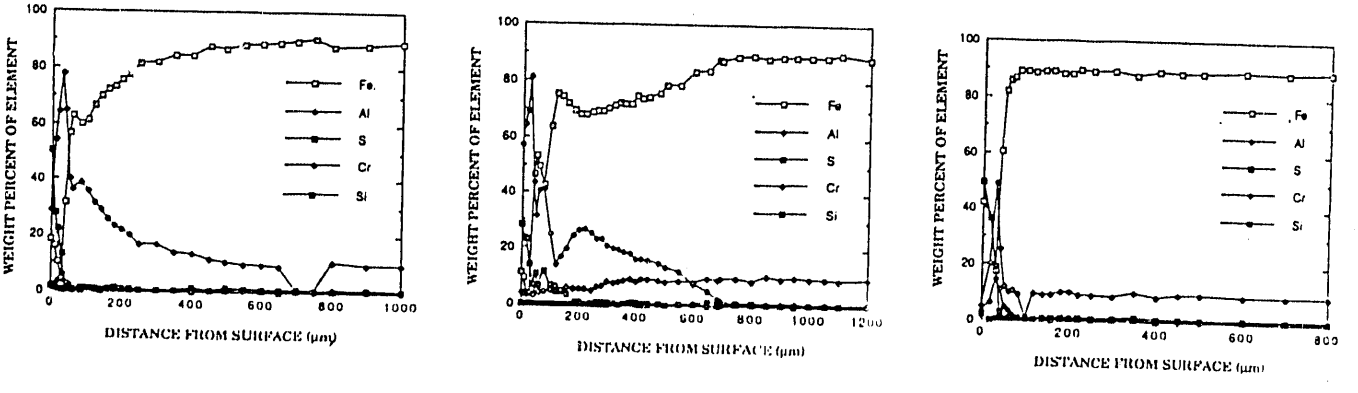

Figure 11. Elemental depth profiles for chromized (left), aluminized (middle), and simultaneously chromized/aluminized (right) T91 alloy after 500 h exposure to gas mixture B at 650°C.

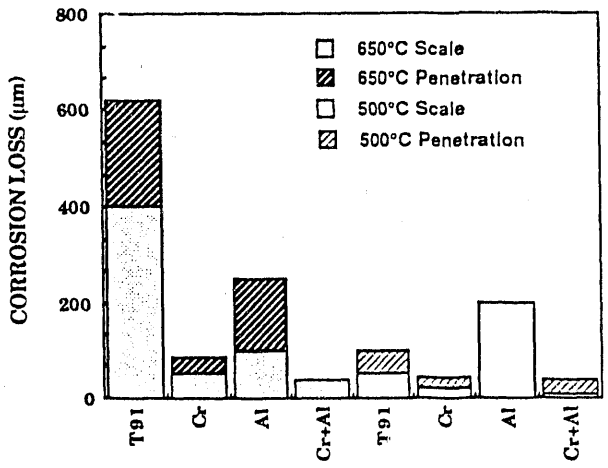

Figure 12. Corrosion loss data for T91 alloy in the uncoated condition and with several coatings after 500 h exposure to gas mixture B at 500 and 650°C.

END

DATE FILMED

12 / 27 / 90